HHS Public Access

Author manuscript

Biosens Bioelectron. Author manuscript; available in PMC 2018 March 15.

Published in final edited form as:

Biosens Bioelectron. 2017 March 15; 89(Pt 1): 400–410. doi:10.1016/j.bios.2016.05.084.

Enhanced Dopamine Detection Sensitivity by PEDOT/Graphene Oxide Coating on in vivo Carbon Fiber Electrodes

I. Mitch Taylor[a], **Elaine M. Robbins**[b], **Kasey A. Catt**[a], **Patrick A. Cody**[a], **Cassandra L. Weaver**[c], and **Xinyan Tracy Cui**[a,*]

[a]University of Pittsburgh, Department of Bioengineering, 3501 Fifth Ave., Pittsburgh, PA 15261, USA

[b]University of Pittsburgh, Department of Chemistry, 219 Parkman Ave., Pittsburgh, PA 15260, USA

[c]University of California, San Diego, Department of Bioengineering, 9500 Gilman Dr., La Jolla, CA 92093, USA

Abstract

Dopamine (DA) is a monoamine neurotransmitter responsible for regulating a variety of vital life functions. In vivo detection of DA poses a challenge due to the low concentration and high speed of physiological signaling. Fast scan cyclic voltammetry at carbon fiber microelectrodes (CFEs) is an effective method to monitor real-time in vivo DA signaling, however the sensitivity is somewhat limited. Electrodeposition of poly(3,4-ethylene dioxythiophene) (PEDOT)/graphene oxide (GO) onto the CFE surface is shown to increase the sensitivity and lower the limit of detection for DA compared to bare CFEs. Thicker PEDOT/GO coatings demonstrate higher sensitivities for DA, but display the negative drawback of slow adsorption and electron transfer kinetics. The moderate thickness resulting from 25 s electrodeposition of PEDOT/GO produces the optimal electrode, exhibiting an 880% increase in sensitivity, a 50% decrease in limit of detection and minimally altered electrode kinetics. PEDOT/GO coated electrodes rapidly and robustly detect DA, both in solution and in the rat dorsal striatum. This increase in DA sensitivity is likely due to increasing the electrode surface area with a PEDOT/GO coating and improved adsorption of DA's oxidation product (DA-o-quinone). Increasing DA sensitivity without compromising electrode kinetics is expected to significantly improve our understanding of the DA function in vivo.

Keywords

Dopamine; PEDOT; Graphene oxide; FSCV; Carbon fiber

*Corresponding author. xic11@pitt.edu.

There are no conflicts of interest.

1. Introduction

Neurochemicals, such as dopamine (DA), are responsible for the regulation of a myriad of physical and cognitive functionality (Brooks 2001; Hull et al. 1999; Urban et al. 2012). Observing the real-time kinetics of in vivo neurochemical signaling is paramount to uncovering these functionalities and furthering our understanding of brain function and dysfunction. Electrochemical methods, such as fast scan cyclic voltammetry (FSCV) and chronoamperometry, have been widely employed for the sub second detection of electroactive neurochemicals such as dopamine (Jones et al. 1995; Kawagoe et al. 1992; Larsen et al. 2011; Taylor et al. 2013; Taylor et al. 2015; Wightman et al. 1988), ascorbic acid (Cofan and Radovan 2008; Yoshimi and Weitemier 2014), norepinephrine (Park et al. 2011), adenosine (Nguyen et al. 2014; Ross et al. 2014) and serotonin (Hashemi et al. 2012; Hashemi et al. 2009; Hashemi et al. 2011). The high temporal resolution afforded by these electrochemical detection techniques allows for in vivo concentration monitoring of neurochemicals on a physiologically relevant timescale (Robinson et al. 2011). Chronoamperometry provides superior temporal resolution but lacks analyte selectivity, while FSCV forfeits temporal resolution for the ability to discern specific analytes via a diagnostic cyclic voltammogram fingerprint. Due to the importance of selectivity, FSCV is often considered a more favorable detection method.

Carbon fiber microelectrodes (CFE) have been used as an electrochemical detector for in vivo neurochemical monitoring for decades (Gonon et al. 1978) due to its efficient electrical conductivity, adsorptive capabilities, and small size (McCreery 2008). In fact, in vivo monitoring of cerebral systems using CFEs has significantly enhanced our understanding of a wide range of cognitive functionalities such as reward (Ambrosi and Pumera 2013), addiction (Phillips et al. 2003a) and motor control (Giros et al. 1996). The use of a small electrode imparts many advantages for in vivo electrochemical detection. First, the small size of the electrode allows for rapid alteration of applied potential. Rapid potential sweeping is necessary for the use of FSCV. Second, the small dimensions of the CFE mitigates damage caused by electrode insertion. The insertion of a 7 μm diameter CFE has been shown to elicit significantly less immune response than a 200 μm diameter microdialysis probe in the rat dorsal striatum (Jaquins-Gerstl and Michael 2009; Peters et al. 2004). It is well documented that the introduction of large foreign bodies into healthy neural tissue elicits a substantial immune response localized to the damage site immediately upon penetration (Borland et al. 2005; Jaquins-Gerstl and Michael 2009; Jaquins-Gerstl et al. 2011; Kozai et al. 2015). This host tissue response disturbs the “healthy” neuronal tissue, subsequently altering the kinetics of neurotransmitter release, uptake, and diffusion (Borland et al. 2005; Mitala et al. 2008; Nesbitt et al. 2013; Nesbitt et al. 2015; Wang and Michael 2012). Third, the small size of the CFE allows for the detection of individual groupings of neurons. This provides the high spatial resolution necessary to map regions of discrete neurotransmitter kinetics throughout the brain (Moquin and Michael 2009; Shu et al. 2013; Taylor et al. 2015). While these features make the CFE an attractive in vivo detector, there is still room for improvement. CFEs exhibit a 200 nM limit of detection and a moderate sensitivity for DA (sensitivity dependent on the length of the exposed carbon fiber). Recent efforts have been made to improve the performance of carbon based electrodes, such as

incorporation of single wall carbon nanotubes onto the CFE surface (Ross and Venton 2012; Swamy and Venton 2007; Xiao and Venton 2012), the development of carbon nanotube fibers and yarns (Jacobs et al. 2014; Schmidt et al. 2013; Zestos et al. 2014; Zestos et al. 2013), the advancement of carbon nanopipettes (Phillips et al. 2003b) and the deposition of conductive polymers and coatings (Gerhardt et al. 1984; Vreeland et al. 2015).

Conductive polymers can be controllably deposited on a substrate surface via the application of a potential sufficient to oxidize and polymerize the specific monomer. The introduction of a thin conductive polymer film increases the effective surface area in addition to incorporating a specific reactive surface on the electrode substrate without sacrificing the conductive property of the electrode. Poly(3,4-ethylene dioxythiophene) (PEDOT) is electro-polymerized from 3,4-ethylene dioxythiophene (EDOT) monomers. The oxidative polymerization of PEDOT results in positive charges on the polymer backbone, this allows for the incorporation of negatively charged doping agents, such as graphene oxide (GO) (Luo et al. 2013a; Wang et al. 2015; Wang et al. 2014; Weaver et al. 2014a; Weaver et al. 2014b), polystyrene sulfonate (PSS) (Alemu et al. 2012; Tait et al. 2013), carbon nanotubes (CNT) (Gerwig et al. 2012; Luo et al. 2011; Xu et al. 2013), Nafion (Vreeland et al. 2015; Wang and Olbricht 2010) and tosylate (Larsen et al. 2012; Vreeland et al. 2014), for the purpose of charge balancing. The introduction of a doping agent also has the added benefit of incorporating additional reactive functional groups. GO, a negatively charged molecule, has great potential in the fields of biosensing, tissue engineering, and drug delivery. The extensive oxidative functionalization of the GO surface inhibits electrical conductivity due to the interruption of conjugated pi bonding (Dreyer et al. 2010). Incorporating GO into the PEDOT conductive polymer coating as a dopant allows for it to be used in an electrode material without the associated drawbacks of an electrical insulator.

PEDOT functionalized materials are widely used as electrochemical sensors (Nie et al. 2013; Zhang et al. 2014; Zhang et al. 2015). In particular, PEDOT/GO and its PEDOT/reduced GO counterpart have been shown to be effective for the selective chemical sensing of DA on 3mm diameter glassy carbon macroelectrodes using conventional cyclic voltammetry (100 mV/s sweep rate) (Wang et al. 2014; Weaver et al. 2014b). In addition, PEDOT/GO coatings can undergo controlled drug delivery upon the application of a trigger potential (Weaver et al. 2014a) or be functionalized to promote cellular interactions for tissue engineering applications (Luo et al. 2013b). These factors make PEDOT/GO a desired coating for CFE modification.

2. Materials and Methods

Carbon fiber electrodes

Single carbon fibers (7 μm diameter, T650; Cytec Carbon Fibers LLC, Piedmont, SC, USA) were thread into borosilicate glass capillaries (0.4 mm ID, 0.6 mm OD; A-M systems Inc., Sequim, WA, USA) and pulled to a fine tip (8 μm OD) using a vertical electrode puller (Narishige puller, Los Angeles, CA, USA). Electrode tips were sealed using low viscosity epoxy (Spurr Epoxy; Polysciences Inc., Warrington, PA, USA). The exposed carbon fibers were trimmed to 400 μm length and electrical connection was established via a drop of mercury and a single nichrome wire (annealed nichrome; Goodfellow, Oakdale, PA, USA).

Fully assembled electrodes were soaked in isopropanol (Bath et al. 2000) for 15 minutes prior to bare electrode calibration, prior to PEDOT/GO coating and prior to calibration post PEDOT/GO coating.

GO synthesis and PEDOT/GO electropolymerization

GO was synthesized via the modified Hummer's method used in previous work (Hummers and Offeman 1958; Luo et al. 2013a; Weaver et al. 2014a; Weaver et al. 2014b) and stored as a concentrated stock in water until use. Prior to use, GO was diluted to 5 mg/mL with water and spiked with 1 μL/mL EDOT monomer. The EDOT/GO solution was stirred vigorously overnight at 4°C prior to 60 minutes (Weaver et al. 2014b) of continuous probe sonication. Probe sonication serves to mechanically exfoliate the GO nanosheets, altering the size and thickness of the GO nanoparticles (Weaver et al. 2014a; Weaver et al. 2014b), in addition to aiding the dissolution of the EDOT monomer. The EDOT/GO solution was prepared in an aqueous solution in the absence of salt to ensure that GO was the sole dopant (Luo et al. 2013a). Conductivity within the EDOT/GO solution was maintained by the presence of negatively charged GO molecules. PEDOT/GO films were electrochemically deposited onto CFE surfaces via chronopotentiometry using a three electrode setup (isopropanol soaked CFE: working, Pt sheet: counter, Ag/AgCl wire: reference) at a Gamry potentiostat, FAS2 femtostat (Gamry Instruments, Warminster, PA, USA). Chronopotentiometry consisted of a single current step from 0 to 12.55 nA for a period of 5, 10, 25, 50, or 100 seconds. Coated electrodes were rinsed in water and soaked in isopropanol for 15 minutes prior to calibration. The reference electrode was stable upon repeated polymerizations, both within and between days, when stored in 1M KCl between uses. Electrochemical impedance measurements were collected from n=3 individual electrodes from each PEDOT/GO deposition duration condition in PBS using a three electrode setup (PEDOT/GO coated CFEs: working, Pt sheet: counter, glass enclosed Ag/AgCl: reference) at an Autolab potentiostat/galvanostat PGSTAT128N (Metrohm, Herisau, Switzerland). Impedance values were in response to a series of 15 mV sinusoidal alternating currents applied in a frequency range between 1 Hz and 100,000 kHz.

Fast scan cyclic voltammetry

FSCV was performed using a two electrode system (CFE: working, glass enclosed Ag/AgCl: reference) at a locally built potential driver (University of Pittsburgh Electronics Shop, Pittsburgh, PA, USA) and a Keithley 428 current amplifier (Keithley Instruments, Cleveland, OH, USA) controlled by the CV Tar Heels LabVIEW program (CV Tar Heels v4.3, courtesy of Dr. Michael Heien, University of Arizona, Tucson, AZ, USA). The potential waveform consisted of a 400 V/sec sweep from the 0 V resting potential up to +1.0 V, down to −0.5 V, and back to the 0 V resting potential applied at 10 Hz. DA detection was confirmed via identification of the background subtracted cyclic voltammogram. The current corresponding to the maximum oxidation potential for each electrode was used to produce the associated current vs. time plots (IT plots). Maximum IT currents were used to generate sensitivity plots and associated sensitivity values. At no point did the potential reach a sufficiently negative potential required to induce reduction of GO to reduced GO (rGO) (Ambrosi and Pumera 2013; Wang et al. 2015; Wang et al. 2014).

Electrode calibration

Electrodes were calibrated using freshly prepared DA HCl (Sigma Aldrich, St. Louis, MO, USA) standards (0.5, 1, 5, and 10 μM) dissolved in N_2 purged artificial cerebral spinal fluid (aCSF: 142 mM NaCl, 1.2 mM $CaCl_2$, 2.7 mM KCl, 1.0 mM $MgCl_2$, 2.0 mM NaH_2PO_4, pH7.4). Calibrations were conducted before (pre-calibration) and after electrodeposition of PEDOT/GO (post-calibration) using a custom built gravity fed flow cell. The apparatus consists of a sample injection port, 500 μL sample loop, waste port, gravity driven aCSF introduction port, and a flow-through detection channel controlled by a pneumatically actuated 6-port valve (Rheodyne 50/5701, Cotati, CA, USA). Electrode sensitivities were determined as the slope of the concentration vs. maximum current plot over the 0.5–10 μM concentration range.

In vivo procedures

All animal procedures were approved by the University of Pittsburgh Institutional Animal Care and Use Committee. Male Sprague Dawley rats (250–350 g: Hilltop Labs, Scottsdale, PA, USA) were anesthetized with isoflurane (2.5% by volume) and were immobilized in a stereotaxic frame with the incisor bar raised to 5 mm above the interaural line (Pellegrino et al. 1979). Body temperature was maintained at 37°C using an internal temperature controlled thermal blanket (Harvard Apparatus, Holliston, MA, USA). Three portions of skull and dura were removed for the introduction of reference, stimulating and working electrodes. Bare or PEDOT/GO coated CFEs were lowered into the dorsal striatum (2.5 mm anterior to bregma, 2.5 mm lateral from bregma and 5 mm below the cortical surface), the bipolar stainless steel reference electrode (MS303/a; Plastics One, Roanoke, VA, USA) was positioned over the medial forebrain bundle (MFB; 2.2 mm posterior to bregma, 1.6 mm lateral from bregma and 7–8.5 mm below the cortical surface: final vertical position adjusted to evoke maximum DA release in the ipsilateral striatum (Ewing et al. 1983; Kuhr et al. 1984; Stamford et al. 1988)) and electrical connection was established between the brain and Ag/AgCl reference electrode via a salt bridge. *In vivo* DA release was achieved through stimulation of the MFB via the application of an optically isolated stimulus waveform (Neurolog 800, Digitimer, Letchworth Garden City, UK) consisting of a biphasic, constant-current square wave (2 ms per pulse, 250 μA pulse height, 60 Hz frequency, 3 second duration) with the aforementioned twisted bipolar stainless steel reference electrode. Further detail of *in vivo* procedures can be found in the following review articles (Robinson et al. 2003; Wightman et al. 1988).

Data analysis

Data was analyzed using MATLAB (MathWorks Inc., Natick, MA, USA) and Microsoft Excel. Statistical analyses were conducted using IBM SPSS software (v22, IBM Corp, Armonk, NY, USA).

Scanning electron microscopy

CFEs were imaged with and without 25 and 100 second PEDOT/GO coating using scanning electron microscopy. SEM images were conducted at the Center For Biologic Imaging at The University of Pittsburgh using a JSM6330 (Jeol, Peabody, MA, USA). Samples were

mounted to the stage and grounded using conductive copper tape. Acceleration voltage used was 3kV and working distance was adjusted automatically for optimal image quality.

3. Results and Discussion

PEDOT/GO Electrodeposition on CFEs

GO was synthesized as in previous studies using the modified Hummers method (Hummers and Offeman 1958; Luo et al. 2013a; Weaver et al. 2014a; Weaver et al. 2014b). Electrodeposition was carried out using an aqueous solution of GO and EDOT in the absence of salt to ensure that GO was the lone dopant molecule (Luo et al. 2013a). Single 7 μm diameter, 400 μm length CFEs were coated with various thicknesses of a PEDOT/GO surface layer by altering the duration of chronopotentiometry electrochemical deposition. Figure 1 displays the scanning electron microscopy (SEM) images of a bare carbon fiber (a) as well as a CFE subjected to 25 s (b) and 100 s (c) of PEDOT/GO electrodeposition (see methods for chronopotentiometry parameters). Figure 1a shows the deep ridge morphology inherent to the graphene based carbon fiber. These ridges aid in the use of carbon fibers as an electrode material by increasing the effective surface area available for electron transfer (Bard and Faulkner 2001). In addition, since the surface of the carbon fiber has been shown to carry a net negative charge due to the presence of oxygen containing functional groups on the edges of graphene subunits (McCreery 2008), the increase in surface area afforded by the deep ridges serves to increase total negative charge on the electrode surface thus improving the adsorption of positivity charged molecules, such as DA (Bath et al. 2001; Bath et al. 2000).

Similarly to the electrodeposition of PEDOT/GO onto glassy carbon electrodes (Luo et al. 2013a; Wang et al. 2015; Wang et al. 2014; Weaver et al. 2014b) and gold substrates (Tian et al. 2014), Figures 1b and c show that PEDOT/GO deposits on the CFE surface as a thin film exhibiting pronounced folds and ridges. These pronounced white folds throughout the coating are believed to be the protrusions of larger GO sheets out of the polymer surface, accompanied by GO's associated negative charge (Tian et al. 2014; Weaver et al. 2014b). Increasing the electrodeposition duration from 25 s (Figure 1b) to 100 s (Figure 1c) appears to increase the density of the pronounced GO folds while further filling the deep inherent CFE ridges. This produces competing effects on the electrode surface area. The filling of the CFE ridges serves to decrease surface area, while the incorporation of additional GO folds act to increase surface area. Using these identical sample preparation/deposition conditions Weaver et al. (2014) determined the oxygen/sulfur ratio for PEDOT/GO to be approximately 12:1. This is a marked enhancement over the fixed 2:1 O/S ratio exhibited by undoped PEDOT polymer, further exhibiting the significant GO doping. Furthermore, during all electrochemical experiments the applied potential did not at any time reach a sufficiently negative potential required to induce reduction of GO to reduced GO (rGO) (Ambrosi and Pumera 2013; Wang et al. 2015; Wang et al. 2014). Electrochemical impedance measurements (Figure 2) of PEDOT/GO coated CFEs reveal that increasing deposition duration decreases impedance over a wide range of sinusoidal current frequencies (Figure 2a). Furthermore, the impedance at 1 kHz is significantly altered by PEDOT/GO deposition duration. This inverse relationship between impedance and PEDOT/Go deposition duration

is likely due to lengthier durations resulting in increased electrode surface area. Further detailed material characterization of PEDOT/GO coatings can be found in our previous manuscripts (Wang et al. 2015; Wang et al. 2014; Weaver et al. 2014b).

Electrochemical Detection of DA Using FSCV

CFEs subjected to 5, 10, 25, 50, or 100 s of PEDOT/GO electrodeposition were evaluated as DA sensing electrodes using 400 V/s FSCV. *In vivo* DA fluctuations occur on the sub-second timescale and the physiologically relevant micromolar concentration range (Taylor et al. 2013; Taylor et al. 2012); subsequently the testing paradigm was designed to mimic such constraints. Electrodes were tested using a user defined, pneumatically actuated flow cell designed to rapidly introduce and remove preloaded DA standards. This addition and subtraction of DA as a concentrated bolus allows for the assessment of DA induced faradaic current as well as adsorption/desorption and electron transfer kinetics (Bath et al. 2001; Bath et al. 2000). Sensor selectivity for DA was confirmed through the examination of background subtracted cyclic voltammograms (CVs). The oxidation/reduction peak potentials remain unchanged for a given analyte at a given set of FSCV collection parameters and serves as a diagnostic fingerprint to confirm selectivity. We have previously displayed the selectivity of PEDOT/GO coatings for DA over common in vivo interferent molecules (i.e. ascorbic acid) (Wang et al. 2014; Weaver et al. 2014b) and in this study further exhibit selective evoked DA detection in vivo.

PEDOT/GO Induced Increase in Capacitive Charging Current

The rapid 400 V/s potential sweep employed by FSCV induces a large non faradaic charging current caused by the formation of an electric double layer on the electrode surface (Bard and Faulkner 2001). As an electrode becomes increasingly charged (either positively or negatively), oppositely charged ions in solution align along the electrode surface forming a temporary capacitor. The subsequent charging and discharging of this electric double layer induced by the FSCV potential waveform sweep produces a stable non faradaic capacitive charging current defined by Equation 1.

$$i_{cap} = ACv \quad \text{(Equation 1)}$$

The non faradaic capacitive charging current, i_{cap}, is defined by the electrode surface area, A, the induced capacitance, C (related to the amount of charge accumulation on the electrode surface) and the potential waveform scan rate, v (Bard and Faulkner 2001).

Figure 3a reveals the average non faradaic charging current associated with the 400 V/s FSCV waveform sweep for CFEs before (n=32, blue) and after 5 s (n=5, red), 10 s (n=5, green), 25 s (n=12, purple), 50 s (n=5, orange), and 100 s (n=5, teal) PEODT/GO electrodeposition. The non faradaic capacitive charging current increases with PEDOT/GO deposition duration from 5 to 100 s. Statistical analysis of the average (±SEM) amplitude of the charging current (Figure 3b) confirms that this increase is highly significant (two-way repeated measures ANOVA, PEDOT/GO: $F(1,27)=13496$, $p<1E^{-38}$, deposition time: $F(4,27)=618$, $p<5E^{-26}$, interaction: $F(4,27)=2069$, $p<5E^{-33}$). Bonferroni post-hoc analysis of

the PEDOT/GO coated electrode groups confirms that all five deposition durations exhibit significantly different ($p<0.05$) average charging current amplitudes. Comparing the same electrodes before and after PEDOT/GO coating removes any error that may be caused by subtle variations between CFEs, thus allowing for direct analysis of the effect of the PEDOT/GO coating.

Based on Equation 1, the increase in non faradaic capacitive charging current detailed in Figure 3 indicates that the PEDOT/GO coating increases either the surface area, capacitance (amount of fixed charge), or both. Analysis of non faradaic charging current alone cannot discern the extent to which each factor contributes, but examination of Figure 1 suggests that both increased surface area and increased charge (due to the incorporation of the negatively charged GO dopant) likely contribute to the observed effect.

Increased DA Sensitivity Resulting from PEDOT/GO Coating

Figure 4a displays (over the same group of electrodes as above) the average current versus time plots (IT plots) in response to a 10 μM DA flow cell challenge. The average maximum faradaic current response to 10 μM DA increases with the PEDOT/GO deposition duration from 5 to 50 s but fails to increase from 50 to 100 s. The sensitivity of each electrode was calculated by determining the linear regression slope of maximum faradaic current versus DA concentration calibration plots over the 0.5 to 10 μM DA concentration range. The average calibration plots (±SEM) including linear regression fits for each group are displayed in Figure 4b and the resulting average (±SEM) sensitivity values are detailed in Figure 4c. Figure 4c displays the average sensitivities for each group of electrodes before (blue) and after (colors detailed in figure legend, n-values described above) PEDOT/GO deposition. Similarly to the trend displayed in Figure 4a, the average CFE sensitivity for DA significantly increases with PEDOT/GO deposition time (two-way repeated measures ANOVA, PEDOT/GO: $F(1,27)=2587$, $p<5E^{-28}$, deposition time: $F(4,27)=53.4$, $p<2E^{-12}$, interaction: $F(4,27)=151$, $p<5E^{-18}$). Bonferroni post-hoc analysis of the PEDOT/GO coated electrodes reveals that the average sensitivities for each deposition duration are significantly different ($p<0.05$) from each other with the exception of the 50 s and 100 s deposition durations which do not exhibit significantly different sensitivities ($p>0.05$). Normalization of the PEDOT/GO sensitivities to their corresponding bare CFE sensitivities provides the average (±SEM) percent sensitivity increase (Table 1). The average percent increase in CFE sensitivity for DA ranges from 295 ± 29 % for a 5 s deposition duration to 1141 ± 108 % for a 50 s deposition of PEDOT/GO.

The lower limit of detection (LOD), defined as the concentration at which the current corresponds to three times the standard deviation of a blank sample (Harris 2003), was determined for each individual electrode before and after PEDOT/GO coating in buffer prior to the introduction of DA. The average (± SEM) LOD for each PEDOT/GO deposition duration is reported in Table 1. PEDOT/GO coating significantly decreases the LOD for DA independent of deposition duration (two-way repeated measures ANOVA, PEDOT/GO: $F(1,27)=45.0$, $p<5E^{-7}$) from 0.218 ± 0.020 μM for bare electrodes to DA concentrations below 0.1 μM for PEDOT/GO deposition durations of 10 s and above. A trend exists toward

decreased LOD as the deposition duration increases, but Bonferroni post-hoc analysis reveals that this trend is not significant ($p>0.05$).

The observed increase in sensitivity and decrease in LOD is comparable to similar work conducted by Vreeland *et al.* (Vreeland et al. 2015) detailing the development of a PEDOT/Nafion coated cylindrical CFE. Our bare CFEs exhibited a lower baseline sensitivity for DA (4.9 ± 0.5 nA/μM) than Vreeland's PEDOT/Nafion electrodes (13 ± 2 nA/μM) but increased to sensitivities (14–54 nA/μM) exceeding those presented for PEDOT/Nafion CFEs (26–46 nA/μM). The lower baseline sensitivities observed for the bare CFEs in this study result in a much larger percent increase in DA sensitivity for PEDOT/GO coated electrodes (295–1106%) compared to PEDOT/Nafion electrodes (200–350%). The LOD for DA presented by Vreeland *et al.* for their bare CFEs (20 ± 7 nM) is an order of magnitude lower than the bare CFE LOD presented in this study (218 ± 20 nM). Since both studies prepare their bare CFEs similarly (Robinson et al. 2003; Vreeland et al. 2015), the discrepancy in bare electrode sensitivity and LOD between Vreeland and our work is likely due to differences in the experimental design. Vreeland et al. use an "optimized potential waveform", scanning from a holding potential of −0.4 V to 1.3V and back at 400 V/s. Combining overoxidation of the electrode by scanning to higher potentials with lowering the electrode holding potential increases the sensitivity and decreases the LOD of the bare CFE for DA (Heien et al. 2003). Due to the susceptibility of PEDOT/GO to overoxidation, we chose the more conservative potential waveform, scanning from a 0 V resting potential up to +1.0 V, down to −0.5 V, and back to the 0 V at 400 V/s. Vreeland's PEDOT/Nafion CFEs lower the LOD for DA (20–30%) to a slightly lower percent of the bare CFE LOD compared to PEDOT/GO CFEs (57–39%). In both cases, incorporation of PEDOT-based conductive polymer coatings onto CFEs enhances the detection capability for DA.

Analysis of Background Subtracted CV Peaks

The faradaic currents measured for each DA standard were confirmed to be due to DA via analysis of the average background subtracted CVs. Figure 5a displays the average CV traces corresponding to the detection of 10 μM DA for each electrode group after subtracting the non faradaic capacitive charging current. Due to the aforementioned stability of the non faradaic charging current, this background subtraction is entirely justified and routine. Each electrode group exhibits characteristic anodic DA oxidation and cathodic dopamine o-quinone (DAoQ) reduction peaks, confirming the detection of DA. Analysis of the ratio of the peak cathodic current ($i_{p,c}$) to the peak anodic current ($i_{p,a}$) as well as the separation of the cathodic and anodic peaks (ΔE_p) reveals interesting details regarding electrode performance. Prior to PEDOT/GO coating, the average (±SEM) $i_{p,c}/i_{p,a}$ ratio (Figure 5b) was 0.56 ± 0.01 over all 32 bare electrodes, indicating that the anodic DA oxidation peak is larger than the cathodic DAoQ reduction peak. The average $i_{p,c}/i_{p,a}$ ratio is significantly increased by the PEDOT/GO coating (two-way repeated measures ANOVA, PEDOT/GO: $F(1,27)=3264$, $p<2E^{-29}$, duration: $F(4,27)=135$, $p<5E^{-17}$, interaction: $F(4,27)=18.3$, $p<5E^{-7}$). In fact, each of the five PEDOT/GO deposition duration groups exhibits an average $i_{p,c}/i_{p,a}$ ratio greater than 1.0, meaning that the cathodic DAoQ reduction peak is larger than the anodic DA oxidation peak in the presence of PEDOT/GO.

The ΔE_p peak separation (Figure 5c) was also significantly altered by the PEDOT/GO deposition (two-way repeated measures ANOVA, PEDOT/GO: $F(1,27)=12.9$, $p<0.002$, duration: $F(4,27)=128$, $p<5E^{-17}$, interaction: $F(4,27)=134$, $p<5E^{-17}$). The average (±SEM) ΔE_p of the bare CFEs was 0.76 ± 0.03 V. The 5 s deposition duration caused both the anodic and cathodic peaks to shift closer to each other, resulting in an average ΔE_p of 0.58 ± 0.01 V. As the PEDOT/GO deposition duration increased from 5 s, the peak separation significantly increased (Bonferroni post-hoc analysis, $p<0.05$) to a maximum average ΔE_p of 1.15 ± 0.01 resulting from the 100 s PEDOT/GO coated electrodes. The 5 and 10 s PEDOT/GO deposition duration electrodes exhibit a significantly smaller ΔE_p than their corresponding bare CFE responses, the 50 and 100 s PEDOT/GO deposition duration electrodes demonstrate a significantly larger ΔE_p than their response prior to coating, and the 25 s deposition does not show a significant deviation in ΔE_p from bare CFE (Bonferroni post hoc analysis).

Mechanism for DA Signal Enhancement

The alteration of peak height and location provides meaningful insight that the mechanism underlying the increase in DA sensitivity caused by PEDOT/GO is due to more than just an increase in electrode surface area. The increase in the cathodic DAoQ reduction peak is indicative of enhanced adsorption of the oxidized DAoQ species onto the electrode surface (Bard and Faulkner 2001). When both the oxidized and reduced species are equally attracted to the electrode surface, both molecules are subject to similar mass transport kinetics. Under these conditions, as DA is oxidized to DAoQ on the electrode surface a steep concentration gradient is formed between the electrode surface and the bulk DA solution. This concentration gradient immediately forces DAoQ away from the electrode surface and brings fresh DA from the bulk solution toward the electrode. The migration of oxidized species away from the electrode surface results in a smaller reduction peak and a $i_{p,c}/i_{p,a}$ ratio less than 1.0 (as is the case with bare CFEs). When the oxidized species is adsorbed to the electrode surface with a higher affinity than the reduced form, the subsequent diffusion of the oxidized species away from the electrode surface is not as robust. This results in larger cathodic reduction peaks and increased $i_{p,c}/i_{p,a}$ ratios. In the case of PEDOT/GO, the affinity for DAoQ appears to be such that a pre concentration of DAoQ occurs on the electrode surface prior to reduction resulting in a DAoQ cathodic reduction peak that is larger and more narrow than its corresponding DA anodic oxidation peak (Bard and Faulkner 2001). This increased adsorption of DAoQ onto the electrode surface is likely due to interactions between the quinone and the GO subunits of the coating (Dreyer et al. 2010; Kaminska et al. 2012).

The initial narrowing of anodic and cathodic peak potential positions (decreased ΔE_p) quantified in Figure 5c indicates that PEDOT/GO accelerates electron transfer kinetics. The redox activity of DA occurs through a two electron, two proton transfer (Deakin et al. 1986; Hawley et al. 1967; Laviron 1984; Tse et al. 1976) with the reaction pathway and associated electron transfer kinetics dependent on DA's adsorption to the electrode surface (DuVall and McCreery 1999, 2000). DuVall and McCreery revealed that the adsorption/desorption of DA/DAoQ onto the electrode surface is necessary for the detection of DA (DuVall and McCreery 1999) likely through interactions with oxygen containing surface functional

groups (Downard et al. 1995; DuVall and McCreery 1999). They went on to show that the adsorption/desorption kinetics at a carbon electrode surface alone are unable to explain the large peak current amplitudes observed for the FSCV detection of DA. Instead, they discovered that the electron transfer kinetics for DA are catalyzed by the adsorption of quinone containing species, including DAoQ, onto the carbon electrode surface (DuVall and McCreery 2000). These findings paired with the aforementioned discovery that PEDOT/GO enhances DAoQ adsorption onto the electrode surface explain the reversal of the $i_{p,c}/i_{p,a}$ ratio and the initial narrowing of ΔE_p observed with PEDOT/GO coated CFEs. Furthermore, when combined with the effects of increasing electrode surface area, these findings explain the enhancement in DA sensitivity caused by PEDOT/GO.

Slowed Electron Transfer Kinetics at Longer Deposition Durations

In order for a probe to be considered an optimal in vivo sensor, it must exhibit rapid kinetic features necessary to observe sub second environmental changes. In this case, an FSCV electrode must demonstrate rapid adsorption/desorption and electron transfer kinetics. The bare CFE has been well established as a rapid and effective in vivo DA sensor and will thus be used as a reference for “acceptably fast” electrode kinetics. The rate of DA absorption/desorption is measured by the time necessary to reach maximum/minimum current following the introduction and removal of a concentrated DA bolus (Bath et al. 2001; Bath et al. 2000). Non-adsorbing molecules, such as ascorbic acid, reach current maximum at a bare CFE immediately upon bolus introduction and exhibit a square-shaped IT response. Adsorbing molecules, such as DA, show a prominent “roll-over” feature in the IT curve prior to reaching maximum current that is indicative of the adsorption kinetics. This roll-over feature, observed after the initial linear current increase, increases the time necessary for the electrode to reach maximum current. The more pronounced the roll-over feature, the slower the adsorption kinetics.

Figure 6a displays the average IT plots to a 10 μM DA bolus (previously displayed in Figure 4a) following normalization to maximum current amplitude. Amplitude normalization allows for detailed comparison of signal rise/fall times as well as the roll-over feature for electrodes before and after PEDOT/GO coating. 5 and 10 sec PEDOT/GO deposition duration electrodes exhibit less pronounced roll-over features than bare CFEs, 25 and 50 s deposition duration electrodes exhibit a slightly more pronounced roll-over features than bare electrodes and the 100 s deposition electrodes display a large roll-over feature. The extent to which each PEDOT/GO coating condition alters the adsorption kinetics was quantified through the calculation of the r^2 correlation coefficient comparing normalized IT responses for each electrode before and after PEDOT/GO coating. The average (±SEM) r^2 correlation coefficient values for the electrodes at each deposition duration are displayed in Figure 6c. There is a trend toward greater deviation in adsorption/desorption kinetics as the deposition time increases. In fact, the average r^2 correlation coefficient of the 100 s deposition electrodes is significantly less than each of the other groups (Bonferroni post hoc, $p<0.05$).

As previously described, rapid potential sweep at the CFE surface induces a large non-faradaic capacitive charging current. This capacitive current rapidly reaches its maximum

and holds until the direction of the potential sweep is reversed, triggering an immediate current discharge and subsequent establishment of a new current maximum of the opposite polarity. The time in which the electrode responds to a change in potential sweep direction is governed by the cell time constant, $R_u C_d$, defined as the shortest time in which an electrode responds to a significant perturbation (e.g. change in potential sweep direction) (Bard and Faulkner 2001). For transient experiments (such as in vivo monitoring) the cell time constant must be small compared to the time scale of the measurement to obtain meaningful results. The cell time constant can be assessed by observing the time required for the non faradaic charging current to establish a new maxima (time of vertical transition) following the reversal of the potential sweep direction. Figure 6b displays the average non faradaic capacitive charging currents normalized to maximum current amplitude. The 5 and 10 s deposition duration electrodes reach a steady state current in a similar timescale as the bare CFEs. 25, 50, and 100 s electrodes take increasingly more time to reach steady state current, suggesting an increasingly slower cell time constant. The effect of PEDOT/GO coating duration on the cell time constant was quantified by determining the r^2 correlation coefficient comparing normalized non faradaic capacitive charging current responses for each electrode before and after PEDOT/GO coating. The average (±SEM) r^2 correlation coefficient values for the electrodes at each deposition duration are displayed in Figure 6d. There is a trend toward greater deviation in cell time constant as the deposition time increases. The average r^2 correlation coefficient of the 50 and 100 s deposition electrodes are significantly lower than each of the other groups (Bonferroni post hoc, $p<0.05$).

Determination of the Optimal PEDOT/GO Deposition Duration

Increasing the duration of PEDOT/GO deposition has competing effects on electrode performance. The sensitivity of DA detection increases with deposition duration (Figure 4) while the adsorption and electron transfer kinetics decrease (Figure 6). 5 and 10 s PEDOT/GO deposition duration electrodes actually appear to increase the DA adsorption rate by decreasing the average roll-over in normalized IT plots compared to bare CFEs (Figure 6) but only display a moderate increase in sensitivity (5 s: 295 ± 29%, 10 s: 532 ± 59%). The 50 and 100 s deposition duration electrodes show similarly large increases in DA sensitivity (50 s: 1141 ± 108, 100 s: 1106 ± 116) but significantly slow electron transfer and adsorption kinetics (Figure 6c,d). The 25 s PEDOT/GO deposition duration electrodes exhibit an 880 ± 88% increase in sensitivity for DA without significantly altering the electrode kinetics, making 25 seconds the optimal deposition duration to produce electrodes capable of collecting high speed/high sensitivity DA measurements.

In Vivo DA Detection

25 s PEDOT/GO deposition duration CFEs were tested for in vivo DA detection. Figure 7 shows the average evoked DA overflow response in the dorsal striatum of six individual rats in response to 3 s, 60 Hz MFB stimulations. These responses were confirmed to be DA in origin through examination of background subtracted CV peak positions. The period of MFB stimulation is denoted by the black bar below the response curves. Under these condition, DA is only released during periods of MFB stimulation. The blue trace represents the average response of n=3 bare CFEs and the red trace is the average of n=3 DA responses collected at 25 s deposition duration PEDOT/GO electrodes. The maximum current

amplitude of in vivo DA detection at 25 s PEDOT/GO electrodes is greater than 500% the current recorded from bare CFEs. The 5 fold increase in sensitivity would enable detection of previously unattainable small DA concentration fluctuations thus revealing finer details of dopamine transmission.

4. Conclusions

Electrodeposited PEDOT/GO coating improves the sensitivity and decreases the LOD of the CFE for DA. This signal enhancement is likely due to increased surface area and higher affinity for the DAoQ oxidation product by the PEDOT/GO coating, which has been shown to catalyze electron transfer between DA and the electrode surface (Bath et al. 2001; Bath et al. 2000). Longer PEDOT/GO deposition durations produced coatings with slow adsorption and electron transfer kinetics, resulting in sensors lacking the temporal resolution necessary for real time in vivo measurement. CFEs subjected to 25 s PEDOT/GO electrodeposition exhibit an 880 ± 88% increase in DA sensitivity without significantly altering electrode kinetics, producing electrodes capable of detecting DA in vivo at high speed and high sensitivity. The development of PEDOT/GO coating for CFEs serves as a significant advancement in the field of in vivo DA monitoring. Increasing DA sensitivity without compromising electrode kinetics can allow for better understanding of DA functionality through the detailed analysis of DA transient function in real time. In addition, electrodeposited PEDOT/GO coatings are highly tunable. Coatings can be tailored towards any specific electroactive analyte or concentration range by varying deposition current, size and oxidation state of GO, etc. Furthermore, by combining sensing with the drug release capability of conducting polymer/GO composites (Weaver et al. 2014a), one may create a close-loop system useful for neuroscience research or neural prosthesis applications.

Acknowledgments

Thank you to Dr. Adrian Michael for the use of his laboratory and FSCV instrumentation. Funding provided by NIH National Institute of Health grants R01NS062019, 7R43DA035545-02, 1R43DA036264-01, 1R43AA022030-01 and National Science Foundation grant ERC-0812348.

References

Alemu D, Wei HY, Ho KC, Chu CW. Highly conductive PEDOT:PSS electrode by simple film treatment with methanol for ITO-free polymer solar cells. Energy Environ Sci. 2012; 5(11):9662–9671.

Ambrosi A, Pumera M. Precise Tuning of Surface Composition and Electron-Transfer Properties of Graphene Oxide Films through Electroreduction. Chem Eur J. 2013; 19(15):4748–4753. [PubMed: 23436748]

Bard, AJ.; Faulkner, LR. Electrochemical Methods: Fundamentals and Applications. 2. John Wiley & Sons, Inc; Hoboken, NJ: 2001.

Bath BD, Martin HB, Wightman RM, Anderson MR. Dopamine Adsorption at Surface Modified Carbon-Fiber Electrodes. Langmuir. 2001; 17(22):7032–7039.

Bath BD, Michael DJ, Trafton BJ, Joseph JD, Runnels PL, Wightman RM. Subsecond adsorption and desorption of dopamine at carbon-fiber microelectrodes. Anal Chem. 2000; 72(24):5994–6002. [PubMed: 11140768]

Borland LM, Shi GY, Yang H, Michael AC. Voltammetric study of extracellular dopamine near microdialysis probes acutely implanted in the striatum of the anesthetized rat. J Neurosci Methods. 2005; 146(2):149–158. [PubMed: 15975664]

Brooks DJ. Functional imaging studies on dopamine and motor control. J Neural Transm. 2001; 108(11):1283–1298. [PubMed: 11768627]

Cofan C, Radovan C. Simultaneous Chronoamperometric Sensing of Ascorbic Acid and Acetaminophen at a Boron-Doped Diamond Electrode. Sensors (Basel, Switzerland). 2008; 8(6): 3952–3969.

Deakin MR, Kovach PM, Stutts KJ, Wightman RM. Heterogeneous Mechanisms of the Oxidation of Catechols and Ascorbic Acid at Carbon Electrodes. Anal Chem. 1986; 58(7):1474–1480. [PubMed: 3728997]

Downard AJ, Roddick AD, Bond AM. Covalent modification of carbon electrodes for voltammetric differentiation of dopamine and ascorbic acid. Anal Chim Acta. 1995; 317(13):303–310.

Dreyer DR, Park S, Bielawski CW, Ruoff RS. The chemistry of graphene oxide. Chem Soc Rev. 2010; 39(1):228–240. [PubMed: 20023850]

DuVall SH, McCreery RL. Control of catechol and hydroquinone electron-transfer kinetics on native and modified glassy carbon electrodes. Anal Chem. 1999; 71(20):4594–4602.

DuVall SH, McCreery RL. Self-catalysis by catechols and quinones during heterogeneous electron transfer at carbon electrodes. J Am Chem Soc. 2000; 122(28):6759–6764.

Ewing AG, Bigelow JC, Wightman RM. Direct in vivo monitoring of dopamine released from two striatal compartments in the rat. Science. 1983; 221(4606):169–171. [PubMed: 6857277]

Gerhardt GA, Oke AF, Nagy G, Moghaddam B, Adams RN. Nafion-coated electrodes with high selectivity for CNS electrochemistry. Brain Res. 1984; 290(2):390–395. [PubMed: 6692152]

Gerwig R, Fuchsberger K, Schroeppel B, Link GS, Heusel G, Kraushaar U, Schuhmann W, Stett A, Stelzle M. PEDOT CNT Composite Microelectrodes for Recording and Electrostimulation Applications: Fabrication, Morphology, and Electrical Properties. Front Neuroeng. 2012; 5:8. [PubMed: 22586394]

Giros B, Jaber M, Jones SR, Wightman RM, Caron MG. Hyperlocomotion and indifference to cocaine and amphetamine in mice lacking the dopamine transporter. Nature. 1996; 379(6566):606–612. [PubMed: 8628395]

Gonon F, Cespuglio R, Ponchon JL, Buda M, Jouvet M, Adams RN, Pujol JF. *In Vivo* Electrochemical Determination of Dopamine Release in Rat Neostriatum. Comptes Rendus Hebdomadaires Des Seances De L Academie Des Sciences Serie D. 1978; 286(16):1203–1206.

Harris, DC. Quantitative chemical analysis. 6. W.H. Freeman and Co; New York: 2003.

Hashemi P, Dankoski EC, Lama R, Wood KM, Takmakov P, Wightman RM. Brain dopamine and serotonin differ in regulation and its consequences. Proceedings of the National Academy of Sciences. 2012; 109(29):11510–11515.

Hashemi P, Dankoski EC, Petrovic J, Keithley RB, Wightman RM. Voltammetric Detection of 5-Hydroxytryptamine Release in the Rat Brain. Anal Chem. 2009; 81(22):9462–9471. [PubMed: 19827792]

Hashemi P, Dankoski EC, Wood KM, Ambrose RE, Wightman RM. In vivo electrochemical evidence for simultaneous 5-HT and histamine release in the rat substantia nigra pars reticulata following medial forebrain bundle stimulation. J Neurochem. 2011; 118(5):749–759. [PubMed: 21682723]

Hawley MD, Tatawawa Sv, Piekarsk S, Adams RN. Electrochemical Studies of Oxidation Pathways of Catecholamines. J Am Chem Soc. 1967; 89(2):447. [PubMed: 6031636]

Heien MLAV, Phillips PEM, Stuber GD, Seipel AT, Wightman RM. Overoxidation of carbon-fiber microelectrodes enhances dopamine adsorption and increases sensitivity. Analyst. 2003; 128(12): 1413–1419. [PubMed: 14737224]

Hull EM, Lorrain DS, Du J, Matuszewich L, Lumley LA, Putnam SK, Moses J. Hormone-neurotransmitter interactions in the control of sexual behavior. Behav Brain Res. 1999; 105(1): 105–116. [PubMed: 10553694]

Hummers WS, Offeman RE. Preparation of Graphitic Oxide. J Am Chem Soc. 1958; 80(6):1339–1339.

Jacobs CB, Ivanov IN, Nguyen MD, Zestos AG, Venton BJ. High Temporal Resolution Measurements of Dopamine with Carbon Nanotube Yarn Microelectrodes. Anal Chem. 2014; 86(12):5721–5727. [PubMed: 24832571]

Jaquins-Gerstl A, Michael AC. Comparison of the brain penetration injury associated with microdialysis and voltammetry. J Neurosci Methods. 2009; 183(2):127–135. [PubMed: 19559724]

Jaquins-Gerstl A, Shu Z, Zhang J, Liu YS, Weber SG, Michael AC. Effect of Dexamethasone on Gliosis, Ischemia, and Dopamine Extraction during Microdialysis Sampling in Brain Tissue. Anal Chem. 2011; 83(20):7662–7667. [PubMed: 21859125]

Jones SR, Garris PA, Kilts CD, Wightman RM. Comparison of Dopamine Uptake in the Basolateral Amygdaloid Nucleus, Caudate-Putamen, and Nucleus Accumbens of the Rat. J Neurochem. 1995; 64(6):2581–2589. [PubMed: 7760038]

Kaminska I, Das MR, Coffinier Y, Niedziolka-Jonsson J, Sobczak J, Woisel P, Lyskawa J, Opallo M, Boukherroub R, Szunerits S. Reduction and Functionalization of Graphene Oxide Sheets Using Biomimetic Dopamine Derivatives in One Step. ACS Appl Mater Interfaces. 2012; 4(2):1016–1020. [PubMed: 22214550]

Kawagoe KT, Garris PA, Wiedemann DJ, Wightman RM. Regulation of transient dopamine concentration gradients in the microenvironment surrounding nerve terminals in the rat striatum. Neuroscience. 1992; 51(1):55–64. [PubMed: 1465186]

Kozai TDY, Jaquins-Gerstl AS, Vazquez AL, Michael AC, Cui XT. Brain Tissue Responses to Neural Implants Impact Signal Sensitivity and Intervention Strategies. ACS Chem Neurosci. 2015; 6(1): 48–67. [PubMed: 25546652]

Kuhr WG, Ewing AG, Caudill WL, Wightman RM. Monitoring the stimulated release of dopamine with in vivo voltammetry. I: Characterization of the response observed in the caudate nucleus of the rat. J Neurochem. 1984; 43(2):560–569. [PubMed: 6736965]

Larsen MB, Sonders MS, Mortensen OV, Larson GA, Zahniser NR, Amara SG. Dopamine Transport by the Serotonin Transporter: A Mechanistically Distinct Mode of Substrate Translocation. J Neurosci. 2011; 31(17):6605–6615. [PubMed: 21525301]

Larsen ST, Vreeland RF, Heien ML, Taboryski R. Characterization of poly(3,4-ethylenedioxythiophene):tosylate conductive polymer microelectrodes for transmitter detection. Analyst. 2012; 137(8):1831–1836. [PubMed: 22383043]

Laviron E. Electrochemical Reactions With Protonations at Equilibrium: Part X. The Kinetics of the *p*-Benzoquinone/Hydroquinone Couple on a Platinum Electrode. J Electroanal Chem. 1984; 164(2): 213–227.

Luo X, Weaver CL, Tan S, Cui XT. Pure graphene oxide doped conducting polymer nanocomposite for bio-interfacing. J Mater Chem B. 2013a; 1(9):1340–1348.

Luo X, Weaver CL, Zhou DD, Greenberg R, Cui XT. Highly stable carbon nanotube doped poly(3,4-ethylenedioxythiophene) for chronic neural stimulation. Biomaterials. 2011; 32(24):5551–5557. [PubMed: 21601278]

Luo XL, Weaver CL, Tan SS, Cui XT. Pure graphene oxide doped conducting polymer nanocomposite for bio-interfacing. Journal of Materials Chemistry B. 2013b; 1(9):1340–1348.

McCreery RL. Advanced Carbon Electrode Materials for Molecular Electrochemistry. Chem Rev. 2008; 108(7):2646–2687. [PubMed: 18557655]

Mitala CM, Wang Y, Borland LM, Jung M, Shand S, Watkins S, Weber SG, Michael AC. Impact of microdialysis probes on vasculature and dopamine in the rat striatum: A combined fluorescence and voltammetric study. J Neurosci Methods. 2008; 174(2):177–185. [PubMed: 18674561]

Moquin KF, Michael AC. Tonic autoinhibition contributes to the heterogeneity of evoked dopamine release in the rat striatum. J Neurochem. 2009; 110(5):1491–1501. [PubMed: 19627437]

Nesbitt KM, Jaquins-Gerstl A, Skoda EM, Wipf P, Michael AC. Pharmacological Mitigation of Tissue Damage during Brain Microdialysis. Anal Chem. 2013; 85(17):8173–8179. [PubMed: 23927692]

Nesbitt KM, Varner EL, Jaquins-Gerstl A, Michael AC. Microdialysis in the Rat Striatum: Effects of 24 h Dexamethasone Retrodialysis on Evoked Dopamine Release and Penetration Injury. ACS Chem Neurosci. 2015; 6(1):163–173. [PubMed: 25491242]

Nguyen MD, Lee ST, Ross AE, Ryals M, Choudhry VI, Venton BJ. Characterization of Spontaneous, Transient Adenosine Release in the Caudate-Putamen and Prefrontal Cortex. PLoS One. 2014; 9(1):e87165. [PubMed: 24494035]

Nie T, Xu JK, Lu LM, Zhang KX, Bai L, Wen YP. Electroactive species-doped poly(3,4-ethylenedioxythiophene) films: Enhanced sensitivity for electrochemical simultaneous

determination of vitamins B2, B6 and C. Biosens Bioelectron. 2013; 50:244–250. [PubMed: 23871872]

Park J, Takmakov P, Wightman RM. In vivo comparison of norepinephrine and dopamine release in rat brain by simultaneous measurements with fast-scan cyclic voltammetry. J Neurochem. 2011; 119(5):932–944. [PubMed: 21933188]

Pellegrino, LJ.; Pellegrino, AS.; Cushman, AJ. A Stereotaxic Atlas of the Rat Brain. Plenum Press; New York, NY: 1979.

Peters JL, Miner LH, Michael AC, Sesack SR. Ultrastructure at carbon fiber microelectrode implantation sites after acute voltammetric measurements in the striatum of anesthetized rats. J Neurosci Methods. 2004; 137(1):9–23. [PubMed: 15196823]

Phillips PEM, Stuber GD, Heien M, Wightman RM, Carelli RM. Subsecond dopamine release promotes cocaine seeking. Nature. 2003a; 422(6932):614–618. [PubMed: 12687000]

Phillips PEM, Stuber GD, Heien MLAV, Wightman RM, Carelli RM. Subsecond dopamine release promotes cocaine seeking. Nature. 2003b; 422(6932):614–618. [PubMed: 12687000]

Robinson DL, Venton BJ, Heien MLAV, Wightman RM. Detecting Subsecond Dopamine Release with Fast-Scan Cyclic Voltammetry in Vivo. Clin Chem. 2003; 49(10):1763–1773. [PubMed: 14500617]

Robinson DL, Zitzman DL, Williams SK. Mesolimbic dopamine transients in motivated behaviors: focus on maternal behavior. Frontiers in Psychiatry. 2011:2. [PubMed: 21629835]

Ross AE, Nguyen MD, Privman E, Venton BJ. Mechanical stimulation evokes rapid increases in extracellular adenosine concentration in the prefrontal cortex. J Neurochem. 2014; 130(1):50–60. [PubMed: 24606335]

Ross AE, Venton BJ. Nafion-CNT coated carbon-fiber microelectrodes for enhanced detection of adenosine. Analyst. 2012; 137(13):3045–3051. [PubMed: 22606688]

Schmidt AC, Wang X, Zhu Y, Sombers LA. Carbon Nanotube Yarn Electrodes for Enhanced Detection of Neurotransmitter Dynamics in Live Brain Tissue. ACS Nano. 2013; 7(9):7864–7873. [PubMed: 23941323]

Shu Z, Taylor IM, Michael AC. The dopamine patchwork of the rat nucleus accumbens core. Eur J Neurosci. 2013; 38(8):3221–3229. [PubMed: 23937532]

Stamford JA, Kruk ZL, Millar J. Stimulated limbic and striatal dopamine release measured by fast cyclic voltammetry: anatomical, electrochemical and pharmacological characterisation. Brain Res. 1988; 454(1–2):282–288. [PubMed: 3261616]

Swamy BEK, Venton BJ. Carbon nanotube-modified microelectrodes for simultaneous detection of dopamine and serotoninin vivo. Analyst. 2007; 132(9):876–884. [PubMed: 17710262]

Tait JG, Worfolk BJ, Maloney SA, Hauger TC, Elias AL, Buriak JM, Harris KD. Spray coated high-conductivity PEDOT:PSS transparent electrodes for stretchable and mechanically-robust organic solar cells. Sol Energy Mater Sol Cells. 2013; 110(0):98–106.

Taylor IM, Ilitchev AI, Michael AC. Restricted Diffusion of Dopamine in the Rat Dorsal Striatum. ACS Chem Neurosci. 2013; 4(5):870–878. [PubMed: 23600442]

Taylor IM, Jaquins-Gerstl A, Sesack SR, Michael AC. Domain-dependent effects of DAT inhibition in the rat dorsal striatum. J Neurochem. 2012; 122(2):283–294. [PubMed: 22548305]

Taylor IM, Nesbitt KM, Walters SH, Varner EL, Shu Z, Bartlow KM, Jaquins-Gerstl AS, Michael AC. Kinetic diversity of dopamine transmission in the dorsal striatum. J Neurochem. 2015; 133(4): 522–531. [PubMed: 25683259]

Tian HC, Liu JQ, Wei DX, Kang XY, Zhang C, Du JC, Yang B, Chen X, Zhu HY, NuLi YN, Yang CS. Graphene oxide doped conducting polymer nanocomposite film for electrode-tissue interface. Biomaterials. 2014; 35(7):2120–2129. [PubMed: 24333027]

Tse DCS, McCreery RL, Adams RN. Potential Oxidative Pathways of Brain Catecholamines. J Med Chem. 1976; 19(1):37–40. [PubMed: 1246050]

Urban NL, Slifstein M, Meda S, Xu X, Ayoub R, Medina O, Pearlson G, Krystal J, Abi-Dargham A. Imaging human reward processing with positron emission tomography and functional magnetic resonance imaging. Psychopharmacology (Berl). 2012; 221(1):67–77. [PubMed: 22052081]

Vreeland RF, Atcherley CW, Russell WS, Xie JY, Lu D, Laude ND, Porreca F, Heien ML. Biocompatible PEDOT:Nafion Composite Electrode Coatings for Selective Detection of Neurotransmitters in Vivo. Anal Chem. 2015; 87(5):2600–2607. [PubMed: 25692657]

Vreeland RF, Laude ND, Lambert SM, Heien ML. Microwave-Plasma Dry-Etch for Fabrication of Conducting Polymer Microelectrodes. Anal Chem. 2014; 86(3):1385–1390. [PubMed: 24417474]

Wang P, Olbricht WL. PEDOT/Nafion composite thin films supported on Pt electrodes: Facile fabrication and electrochemical activities. Chem Eng J. 2010; 160(1):383–390.

Wang W, Wang W, Davis J, Luo X. Ultrasensitive and selective voltammetric aptasensor for dopamine based on a conducting polymer nanocomposite doped with graphene oxide. Microchim Acta. 2015; 182(5):1123–1129.

Wang W, Xu G, Cui XT, Sheng G, Luo X. Enhanced catalytic and dopamine sensing properties of electrochemically reduced conducting polymer nanocomposite doped with pure graphene oxide. Biosens Bioelectron. 2014; 58:153–156. [PubMed: 24632460]

Wang Y, Michael AC. Microdialysis probes alter presynaptic regulation of dopamine terminals in rat striatum. J Neurosci Methods. 2012; 208(1):34–39. [PubMed: 22546476]

Weaver CL, LaRosa JM, Luo X, Cui XT. Electrically Controlled Drug Delivery from Graphene Oxide Nanocomposite Films. ACS Nano. 2014a; 8(2):1834–1843. [PubMed: 24428340]

Weaver CL, Li H, Luo X, Cui XT. A graphene oxide/conducting polymer nanocomposite for electrochemical dopamine detection: origin of improved sensitivity and specificity. J Mater Chem B. 2014b; 2(32):5209–5219.

Wightman RM, May LJ, Michael AC. Detection of Dopamine Dynamics in the Brain. Anal Chem. 1988; 60(13):769A–779A.

Xiao N, Venton BJ. Rapid, Sensitive Detection of Neurotransmitters at Microelectrodes Modified with Self-assembled SWCNT Forests. Anal Chem. 2012; 84(18):7816–7822. [PubMed: 22823497]

Xu G, Li B, Cui XT, Ling L, Luo X. Electrodeposited conducting polymer PEDOT doped with pure carbon nanotubes for the detection of dopamine in the presence of ascorbic acid. Sensors Actuators B: Chem. 2013; 188:405–410.

Yoshimi K, Weitemier A. Temporal Differentiation of pH-Dependent Capacitive Current from Dopamine. Anal Chem. 2014; 86(17):8576–8584. [PubMed: 25105214]

Zestos AG, Jacobs CB, Trikantzopoulos E, Ross AE, Venton BJ. Polyethylenimine Carbon Nanotube Fiber Electrodes for Enhanced Detection of Neurotransmitters. Anal Chem. 2014; 86(17):8568–8575. [PubMed: 25117550]

Zestos AG, Nguyen MD, Poe BL, Jacobs CB, Venton BJ. Epoxy insulated carbon fiber and carbon nanotube fiber microelectrodes. Sensors Actuators B: Chem. 2013; 182:652–658.

Zhang K, Xu J, Duan X, Lu L, Hu D, Zhang L, Nie T, Brown KB. Controllable synthesis of multi-walled carbon nanotubes/poly(3,4-ethylenedioxythiophene) core-shell nanofibers with enhanced electrocatalytic activity. Electrochimica Acta. 2014; 137:518–525.

Zhang K, Xu J, Zhu X, Lu L, Duan X, Hu D, Dong L, Sun H, Gao Y, Wu Y. Poly(3,4-ethylenedioxythiophene) nanorods grown on graphene oxide sheets as electrochemical sensing platform for rutin. J Electroanal Chem. 2015; 739:66–72.

Highlights

- We developed a PEDOT/GO coated carbon fiber microelectrode for in vivo use.
- Electrodes exhibit 880% sensitivity increase for dopamine versus bare carbon fiber.

PEDOT/GO electrodes successfully detected electrically stimulated dopamine in vivo.

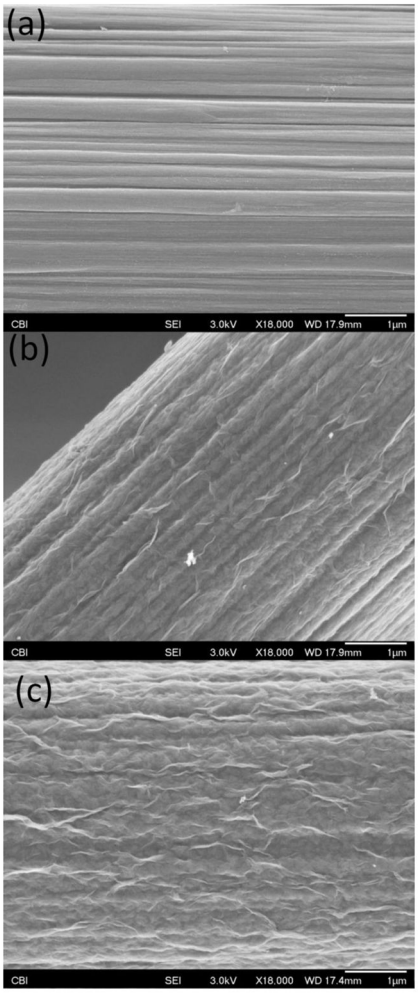

Figure 1.
Scanning electron microscopy images of a bare CFE (a), a 25 s PEDOT/GO coated CFE (b) and a 100 s PEDOT/GO coated CFE (c). All three images display an 18,000X magnification of the electrode surfaces. The scale bars represent 1 μm.

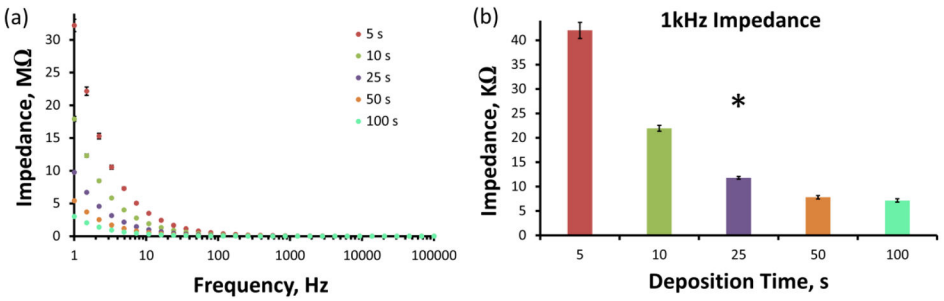

Figure 2.

Electrochemical impedance spectroscopy characterization of PEDOT/GO coated CFEs. (a) Average impedance measurements of (n=3 individual electrodes for each deposition duration) over a 1–100,000 Hz sinusoidal current frequency range. (b) The average impedance at 1 kHz sinusoidal current frequency is significantly altered by PEDOT/GO deposition duration (* one-way ANOVA: $F(4,14)=234$, $p<1e^{-9}$).

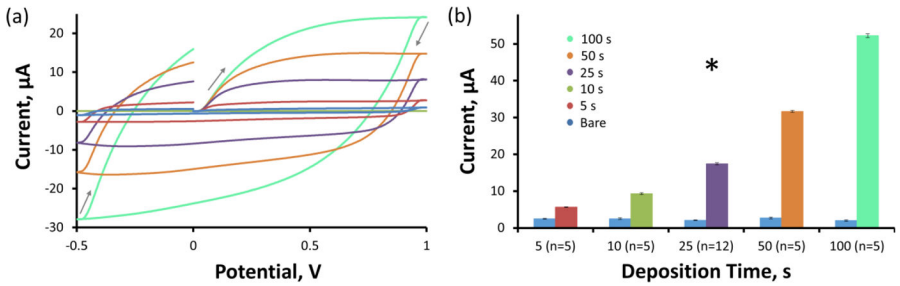

Figure 3.

PEDOT/GO increases the non faradaic current associated with a 400 V/s FSCV scan rate. (a) The average amplitude of the non faradaic current increases with the duration of PEDOT/GO deposition. The grey arrows depict the potential waveform sweep direction. (b) The average (±SEM) total non faradaic charging current amplitude significantly increases with the duration of PEDOT/GO deposition (* two-way repeated measures ANOVA, PEDOT/GO: $F(1,27)=13496$, $p<1E^{-38}$, deposition time: $F(4,27)=618$, $p<5E^{-26}$, interaction: $F(4,27)=2069$, $p<5E^{-33}$).

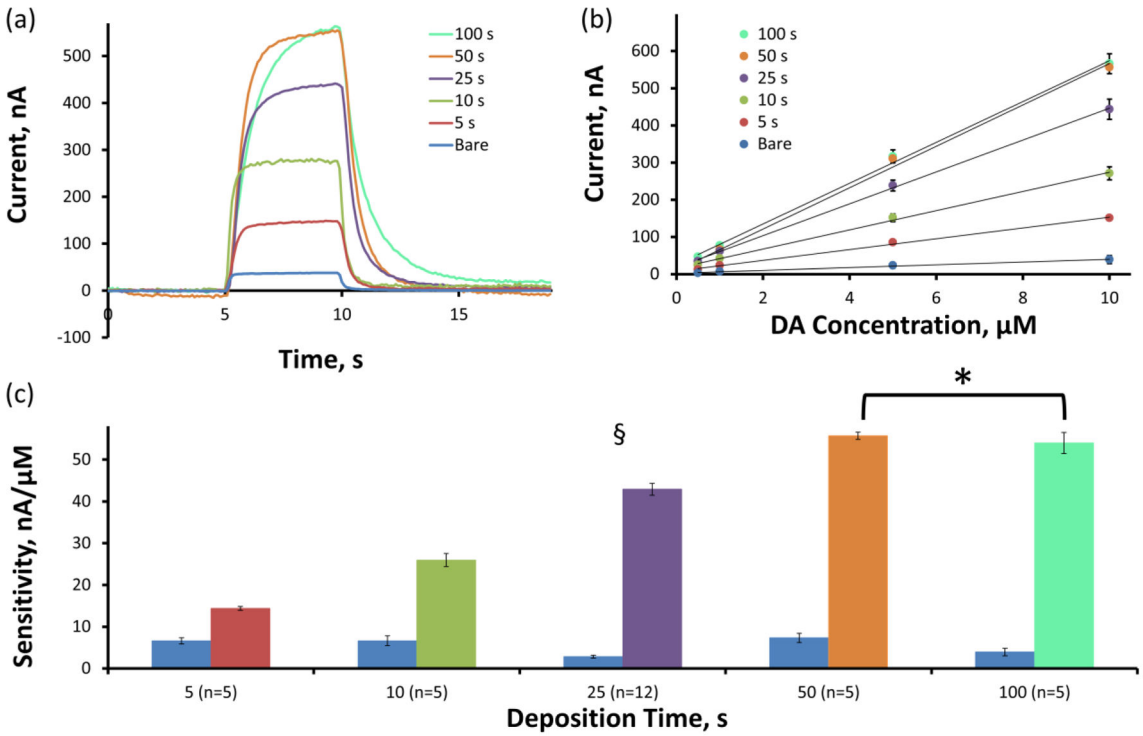

Figure 4.

PEDOT/GO increases the faradaic current associated with the detection of DA using FSCV. (a) The average faradaic current induced by a 10 µM DA challenge increases with the duration of PEDOT/GO deposition. (b) Sensitivity for DA is determined as the slope of the linear regression fit of the concentration versus current calibration plot. (c) The average CFE sensitivity for DA significantly increases with the duration of PEDOT/GO deposition (§ two-way repeated measures ANOVA, PEDOT/GO: $F(1,27)=2587$, $p<5E^{-28}$, deposition time: $F(4,27)=53.4$, $p<2E^{-12}$, interaction: $F(4,27)=151$, $p<5E^{-18}$). Bonferroni post-hoc comparison reveals that sensitivity significantly increases with each increase in deposition time until the increase from 50 to 100 s (* $p>0.05$).

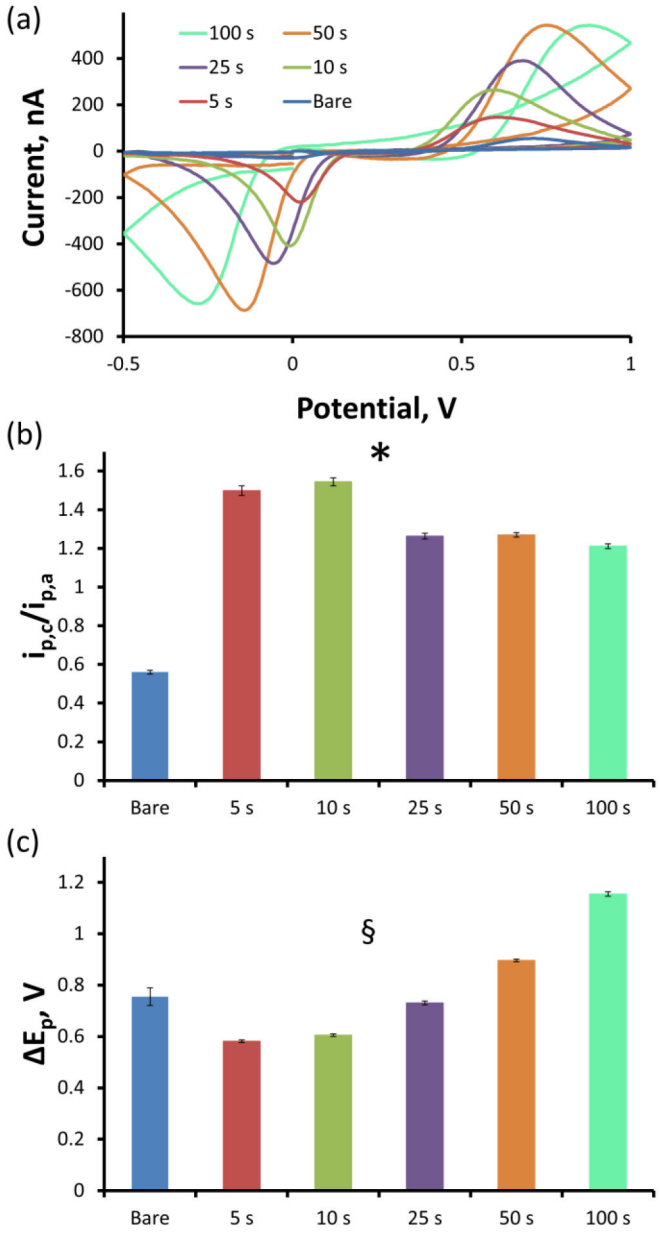

Figure 5.

Both bare and PEDOT/GO CFEs observe the signature DA CV (a) in response to a 10 μM DA challenge, confirming the detection of DA. (b) The $i_{p,c}/i_{p,a}$ ratio is significantly altered by the PEDOT/GO coating and duration (* two-way repeated measures ANOVA, PEODT/GO: $F(1,27)=3264$, $p<2E^{-29}$, duration: $F(4,27)=135$, $p<5E^{-17}$, interaction: $F(4,27)=18.3$, $p<5E^{-7}$). (c) ΔE_p is significantly affected by the PEDOT/GO coating and duration (§ two-way repeated measures ANOVA, PEODT/GO: $F(1,27)=12.9$, $p<0.002$, duration: $F(4,27)=128$, $p<5E^{-17}$, interaction: $F(4,27)=134$, $p<5E^{-17}$).

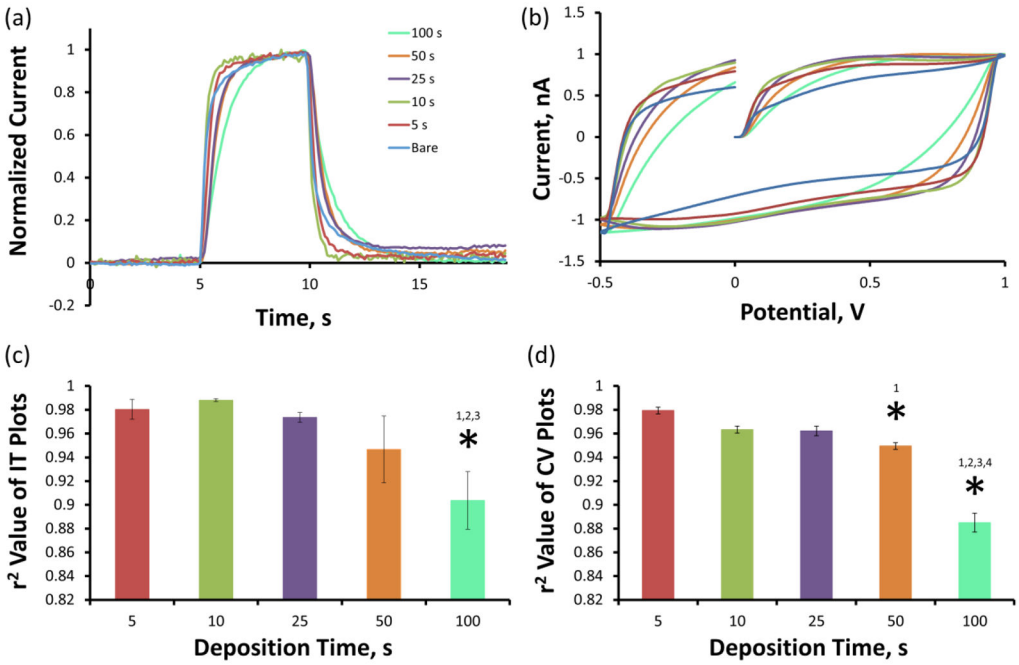

Figure 6.

Longer PEDOT/GO deposition durations slow electrode kinetics. (a) The average IT responses normalized to maximum amplitude reveal that the vertical rise and fall time associated with the introduction and removal of a 10 μM DA bolus increases with deposition time. (b) The average non faradaic charging currents normalized to maximum amplitude also reveal a lag in electron transfer kinetics correlating to PEDOT/GO deposition duration. The extent to which the electrode kinetics are altered is assessed by r^2 correlation coefficient calculation comparing responses pre- and post PEDOT/GO deposition. PEDOT/GO significantly alters the electrode kinetics of the IT plot (c) at 100 s and of the CV plot (d) at 50 and 100s, as measured by the average r^2 correlation coefficients (* one-way ANOVA Bonferroni post hoc, $p<0.05$).

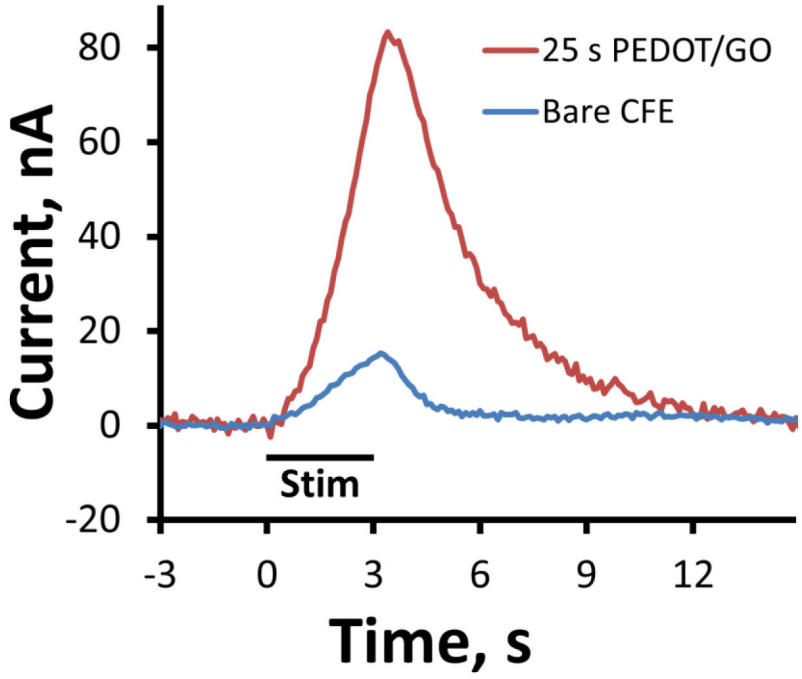

Figure 7.

PEDOT/GO increases the current of in vivo DA detection in the rat dorsal striatum elicited by a 3 s, 60Hz MFB stimulation train. The blue trace is the average evoked DA overflow response of n=3 individual bare CFEs collected from three separate animals. The red trace is the average response from n=3 individual 25 s deposition duration PEDOT/GO electrodes collected from an addition three separate animals. The period of MFB stimulation is denoted by the black bar.

Table 1

Sensitivity increase and LOD of the PEDOT/GO coated CFE. Average (±SEM) percent increase in sensitivity for DA was determined for each deposition duration by comparing post coating sensitivities to the corresponding bare electrode sensitivities (average raw sensitivities displayed in Figure 4c). PEDOT/GO significantly decreases the LOD for DA when the deposition duration exceeds 10 s (* two-way repeated measures ANOVA, PEDOT/GO: $F(1,27)=45.0$, $p<5E^{-7}$).

	Bare (n=32)	**5 (n=5)**	**10 (n=5)**	**25 (n=12)**	**50 (n=5)**	**100 (n=5)**
% Sensitivity Increase		295 ± 29	532 ± 59	880 ± 88	1141 ± 108	1106 ± 116
LOD, μM*	0.218 ± 0.020	0.125 ± 0.009	0.093 ± 0.013	0.090 ± 0.007	0.087 ± 0.015	0.085 ± 0.009